ACS OMEGA

http://pubs.acs.org/journal/acsodf

Article

Kinetic Studies of Hantzsch Ester and Dihydrogen Donors Releasing Two Hydrogen Atoms in Acetonitrile

Yan-Hua Fu,* Cuihuan Geng, Guang-Bin Shen,* Kai Wang, and Xiao-Qing Zhu*

Cite This: *ACS Omega* 2022, 7, 26416−26424

Read Online

ACCESS | Metrics & More | Article Recommendations | Supporting Information

ABSTRACT: In this work, kinetic studies on HEH_2, 2-benzylmalononitrile, 2-benzyl-1*H*-indene-1,3(2*H*)-dione, 5-benzyl-2,2-dimethyl-1,3-dioxane-4,6-dione, 5-benzyl-1,3-dimethylpyrimidine-2,4,6(1*H*,3*H*,5*H*)-trione, 2-(9*H*-fluoren-9-yl)malononitrile, ethyl 2-cyano-2-(9*H*-fluoren-9-yl)acetate, diethyl 2-(9*H*-fluoren-9-yl)malonate, and the derivatives (28 XH_2) releasing two hydrogen atoms were carried out. The thermokinetic parameters $\Delta G^{\ddagger\circ}$ of 28 dihydrogen donors (XH_2) and the corresponding hydrogen atom acceptors ($XH^{\bullet}$) in acetonitrile at 298 K were determined. The abilities of releasing two hydrogen atoms for these organic dihydrogen donors were researched using their thermokinetic parameters $\Delta G^{\ddagger\circ}(XH_2)$, which can be used not only to compare the H-donating ability of different XH_2 qualitatively and quantitatively but also to predict the rates of HAT reactions. Predictions of rate constants for 12 HAT reactions using thermokinetic parameters were determined, and the reliabilities of the predicted results were also examined.

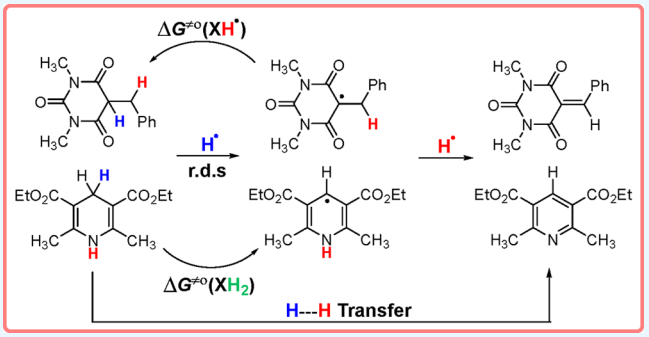

INTRODUCTION

The hydrogenation reaction is one of the most widely studied and applied reactions in organic chemistry, a chemical process in which a reducing agent releases two hydrogen atoms or ions to form an unsaturated bond.[1−3] In our previous work, we have elucidated the differences between Hantzsch ester (HEH_2) and free H_2 gas as reducing agents in thermodynamics, and the related thermodynamic data of HEH_2 and free H_2 gas releasing two hydrogen atoms or ions have been provided.[4] The thermodynamic parameters on 20 possible elementary steps of Hantzsch ester (HEH_2), benzothiazoline (BTH_2), and dihydrophenanthridine (PDH_2) releasing two hydrogen atoms or ions have also been measured or derived from the related thermodynamic data using Hess' law in acetonitrile.[5] These three organic compounds are dihydrogen donors usually used to reduce olefins, aldehydes, ketones, imines, alkynes, and quinolines and have received wide attention owing to their study and application prospects in academia and industry.[6−12] In addition to these three dihydrogen donors, 2-benzylmalononitrile, 2-(9*H*-fluoren-9-yl)malononitrile, 2-benzyl-1H-indene-1,3(2*H*)-dione, 5-benzyl-2,2-dimethyl-1,3-dioxane-4,6-dione, 5-benzyl-1,3-dimethylpyrimidine-2,4,6(1*H*,3*H*,5*H*)-trione, ethyl 2-cyano-2-(9*H*-fluoren-9-yl)acetate, diethyl 2-(9*H*-fluoren-9-yl)malonate, and the derivatives (Scheme 1) are also good dihydrogen donors. They are very popular in synthesis, catalysis, medicinal chemistry, and biochemistry.[13−15] Since they are all good reductants in organic synthesis and industrial production, it is necessary and urgent to study their actual dihydrogen-donating abilities in kinetics quantitatively.

In this work, 28 organic dihydrogen reductants releasing two hydrogen atoms in hydrogen atom transfer (HAT) reactions (eq 1) in acetonitrile are determined, and the thermodynamic and kinetic parameters in the $H^{\bullet}-H^{\bullet}$ donating process are established. The purpose of this work is to elucidate the differences between HEH_2 and dihydrogen donors (XH_2) shown in Scheme 1 as popular reducing agents in thermodynamics, kinetics, and thermokinetics, and to study their abilities of releasing two hydrogen atoms in HAT reactions qualitatively and quantitatively, although the H-donating abilities of dihydrogen donors have been discussed in our previous work.[4,5] However, the H-donating abilities of these compounds were only studied from a thermodynamics viewpoint. In this work, thermodynamic bond dissociation free energy [$\Delta G^{\circ}(XH_2)$], activation free energy of the self-exchange HAT reaction [$\Delta G^{\ddagger}_{XH_2/XH^{\bullet}}$], and the thermokinetic parameter [$\Delta G^{\ddagger\circ}(XH_2)$] are used to compare and analyze the H-donating abilities of these compounds from thermodynamics, kinetics, and actual reaction directions.

$$XH_2 + 2Y^{\bullet} \rightarrow X + 2Y - H \quad (1)$$

Received: April 11, 2022
Accepted: July 6, 2022
Published: July 22, 2022

https://doi.org/10.1021/acsomega.2c02264
ACS Omega 2022, 7, 26416−26424

Scheme 1. Molecular Structures of XH_2 as Two-Hydrogen-Atom Donors Examined in This Work

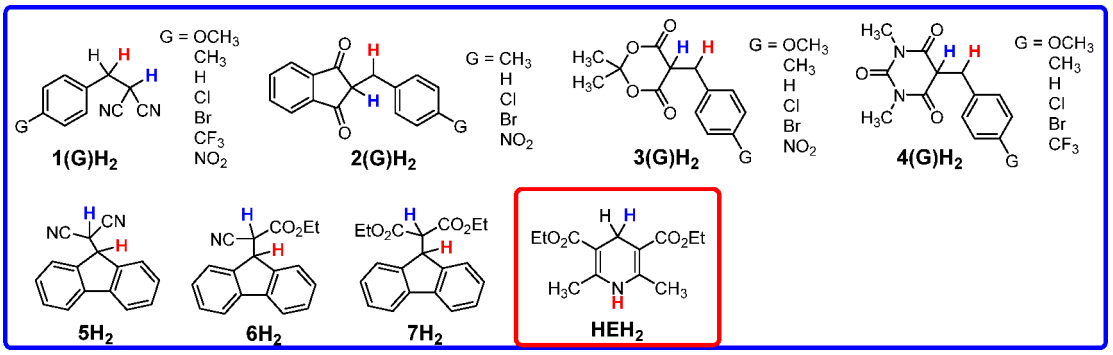

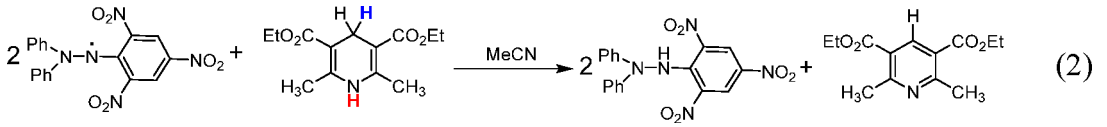

RESULTS AND DISCUSSION

XH_2 shown in Scheme 1 were prepared according to the known synthesis method from the previous literature.[16,19] The structures of XH_2 and X were characterized by ^{1}H NMR spectra in the Supporting Information (SI). The nitrogen-centered radical 2,2-diphenyl-1-picrylhydrazyl (DPPH$^\bullet$) was selected since it was a relatively stable neutral radical and frequently used as a reactive oxygen species (ROS) model to evaluate the radical-scavenging activity of antioxidants. It was extensively employed in kinetic studies of H-abstraction for many antioxidants.[17] Kinetic studies on two-hydrogen-atom transfer reactions between HEH_2 (eq 2) and other dihydrogen donors XH_2 with DPPH$^\bullet$ were carried out by UV−vis stopped-flow spectrophotometry under pseudo-first-order conditions with an excess of XH_2 over DPPH$^\bullet$ in acetonitrile at 298 K. The absorbance decay of DPPH$^\bullet$ at λ_{max} = 518 nm after addition of HEH_2 (Figure 1) in deaerated anhydrous acetonitrile at 298 K was monitored. The thermodynamic analytic platform (TAP) for the reaction mechanism of HEH_2/DPPH$^\bullet$ in acetonitrile was analyzed in Scheme 2, and other XH_2/DPPH$^\bullet$ are shown in the SI. The absorbance decay of $4H_2$/DPPH$^\bullet$ (eq 3) in acetonitrile at λ_{max} = 518 nm (Figure 2) was also monitored under a pseudo-first-order kinetic model. According to the TAP of the reaction mechanism, it is clear that the two hydrogen atoms are releasing as H$^\bullet$−H$^\bullet$ stepp by stepp, and the first HAT is the rate-determining step. After losing one hydrogen atom (the blue one), the intermediate XH$^\bullet$ rapidly loses the other hydrogen atom (the red one), resulting in the stable activated olefin. Thus, the H-donating ability of the dihydrogen donor is determined by how easily the blue hydrogen atom (Scheme 1) is lost. The product analysis was proved by ^{1}H NMR in the SI.

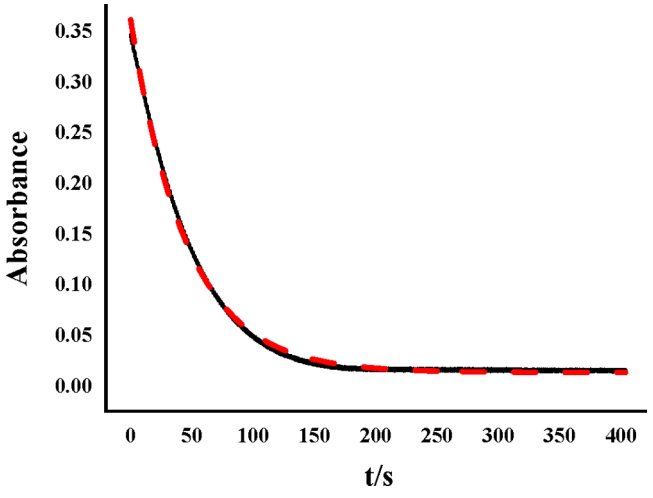

Figure 1. Absorbance decay of DPPH$^\bullet$ (0.1 mM) in acetonitrile at λ_{max} = 518 nm after addition of HEH_2 (2.0 mM) in deaerated anhydrous acetonitrile at 298 K (black line) and the fit (red line) using a pseudo-first-order kinetic model.

In our previous works,[16,18] a new kinetic model (eq 4) was proposed to quantitatively estimate the activation free energy of HAT reaction (eq 1) using only one physical parameter for each reactant. The two parameters on the right of eq 4 are thermokinetic parameters of the two-hydrogen-atom donor (XH_2) and the free radical (Y$^\bullet$); the definitions of both are listed in eqs 5 and 6 according to the new kinetic model. They can be used to evaluate the actual H-donating ability of hydrogen donor $\Delta G^{\ddagger\circ}(XH_2)$ and the actual H-accepting ability of free radical $\Delta G^{\ddagger\circ}(Y^\bullet)$ accurately and quantitatively. In eqs 5 and 6, $\Delta G^\circ(XH_2)$ is the bond dissociation free energy of XH-H, the first hydrogen atom release of which is shown in in Scheme 1. It is the thermodynamic parameter of XH_2, usually used to assess the potential H-donating capacity of XH_2. $\Delta G^{\ddagger}_{XH_2/XH^\bullet}$ is the activation free energy of the self-exchange HAT reaction for XH_2 (XH_2 + XH$^\bullet$ → XH$^\bullet$ + XH_2). That is the kinetic intrinsic resistance as the thermodynamic driving force of the reaction is zero, which means the kinetic intrinsic resistance barrier of XH_2 in the process of releasing the first hydrogen atom (the blue one). It is often called internal resistance energy. Therefore, as long as the thermokinetic parameter of dihydrogen donor is known, it can be used to quantitatively measure the actual H-donating ability of any dihydrogen donor.

$$\Delta G^{\ddagger}_{XH_2/Y^\bullet} = \Delta G^{\ddagger\circ}(XH_2) + \Delta G^{\ddagger\circ}(Y^\bullet) \quad (4)$$

$$\Delta G^{\ddagger\circ}(XH_2) \equiv 1/2[\Delta G^{\ddagger}_{XH_2/XH^\bullet} + \Delta G^\circ(XH_2)] \quad (5)$$

$$\Delta G^{\ddagger\circ}(Y^\bullet) \equiv 1/2[\Delta G^{\ddagger}_{YH/Y} - \Delta G^\circ(YH)] \quad (6)$$

In order to obtain the H-donating abilities of these dihydrogen reductants, in this work, the second-order rate

https://doi.org/10.1021/acsomega.2c02264
ACS Omega 2022, 7, 26416−26424

Scheme 2. Thermodynamic Analytic Platform (TAP) for the Reaction Mechanism of HEH_2 with DPPH• in Acetonitrile[a]

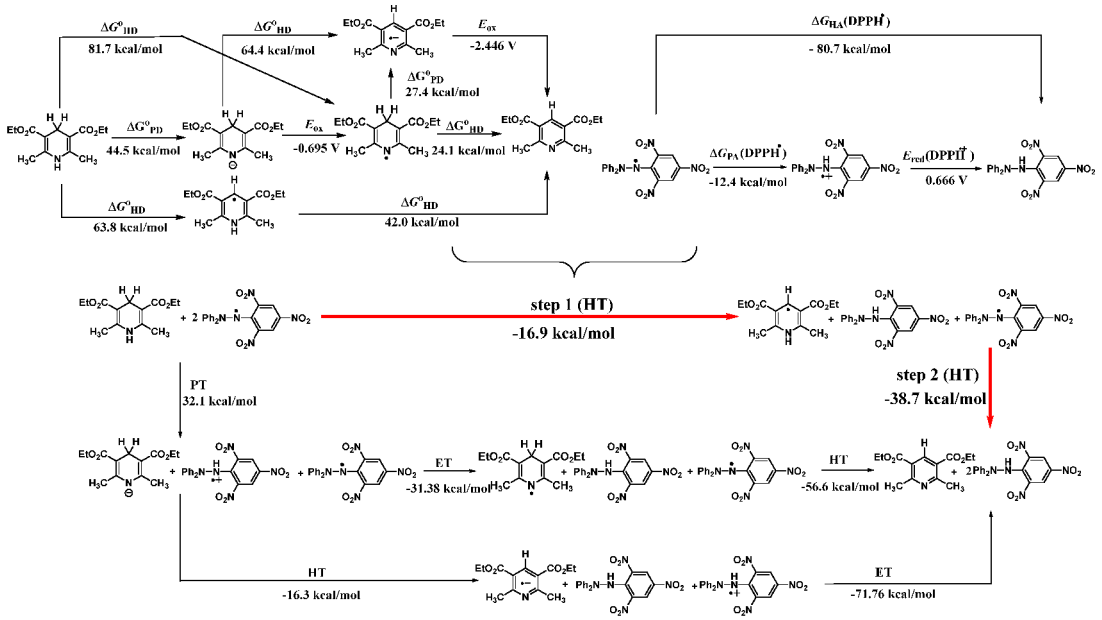

[a]Diagnostic conclusion from TAP: the most likely reaction pathway of HEH_2/DPPH• is shown by red arrows: step 1 (rate-determined).

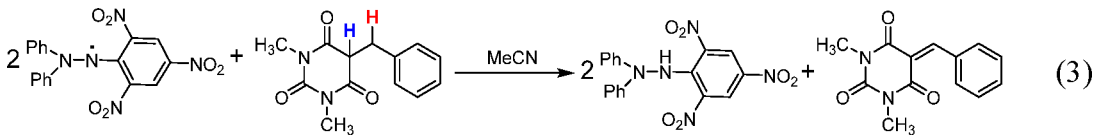

(3)

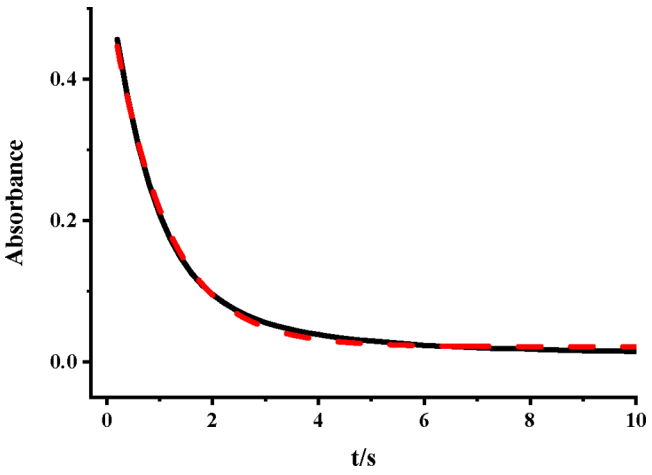

Figure 2. Absorbance decay of DPPH• (0.1 mM) in acetonitrile at λ_{max} = 518 nm after addition of $4H_2$ (2.0 mM) in deaerated anhydrous acetonitrile at 298 K (black line) and the fit (red line) using the pseudo-first-order kinetic model.

constants (k_2) and the corresponding activation free energies ($\Delta G^{\ddagger}_{XH_2/DPPH•}$) of 28 cross HAT reactions (XH_2/DPPH•) in acetonitrile at 298 K were determined, and the detailed results are summarized in Table 1. In order to calculate the thermokinetic parameters of XH_2 and XH• in acetonitrile at 298 K, the molar free energy changes ΔG° of these cross HAT reactions were also provided in Table 1.

Since the thermokinetic parameter $\Delta G^{\ddagger\circ}$(DPPH•) = −29.67 kcal/mol was already obtained in our previous work,[16] the thermokinetic parameters $\Delta G^{\ddagger\circ}(XH_2)$ of these 28 dihydrogen donors could be obtained using eq 4 as $\Delta G^{\ddagger}_{XH_2/DPPH•}$ are shown in Table 1. The results were summarized in Table 2. The $\Delta G^{\ddagger\circ}(XH_2)$ values of these 28 dihydrogen atom donors (XH_2) and the $\Delta G^{\ddagger\circ}(XH•)$ values of the corresponding hydrogen atom acceptors (XH•) in acetonitrile at 298 K can be derived from the corresponding $\Delta G^{\ddagger}_{XH_2/XH•}$ and $\Delta G^{\circ}(XH_2)$ values using eqs 5 and 6, respectively. The results were also listed in Table 2. In order to conveniently calculate $\Delta G^{\ddagger\circ}(XH_2)$ and $\Delta G^{\ddagger\circ}(XH•)$, the $\Delta G^{\circ}(XH_2)$ values in acetonitrile at 298 K which were obtained from ref 19 are also listed in Table 2.

The Scales of Thermokinetic Parameters of Dihydrogen Donors XH_2 and the Corresponding Radicals XH•. From Table 2, it is clear that the $\Delta G^{\ddagger\circ}(XH_2)$ values of 28 dihydrogen donors (XH_2) in acetonitrile at 298 K range from 43.57 kcal/mol for $4(CF_3)H_2$ to 48.43 kcal/mol for $1(OCH_3)$-H_2, and the $\Delta G^{\ddagger\circ}(XH•)$ values of the corresponding hydrogen atom acceptors (XH•) range from −30.47 kcal/mol for $4(OH_3)H•$ to −16.78 kcal/mol for HEH•. In order to make the thermokinetic parameters in Table 2 be convenient for the application, and discover the dependence of $\Delta G^{\ddagger\circ}(XH_2)$ and $\Delta G^{\ddagger\circ}(XH•)$ on the structures and compare the thermokinetic parameters of XH_2 and the corresponding radical intermediates XH• after the loss of one hydrogen atom intuitively, the compounds are sorted according to the value order of thermokinetic parameters in Schemes 3 and 4, respectively.

From Schemes 3 and 4, it is clear that the effects of the structures of XH_2 and XH• on $\Delta G^{\ddagger\circ}(XH_2)$ and $\Delta G^{\ddagger\circ}(XH•)$ are quite enormous. In Scheme 3, it is not difficult to see that the order of thermokinetic parameters $\Delta G^{\ddagger\circ}(XH_2)$ of these dihydrogen donors is $4(G)H_2$ < $2(G)H_2$ < $3(G)H_2$ ($5H_2$ < $6H_2$ < $7H_2$) < HEH_2 < $1(G)H_2$. As discussed in our previous

https://doi.org/10.1021/acsomega.2c02264
ACS Omega 2022, 7, 26416−26424

Table 1. Second-Order Rate Constants (k_2), Activation Free Energies ($\Delta G^{\ddagger}$), and Molar Free Energy Changes (ΔG°) of HAT Reactions XH_2/DPPH$^{\bullet}$ in Acetonitrile at 298 K

entry	XH_2/DPPH$^{\bullet}$		$k_2(M^{-1}s^{-1})$[a]	$\Delta G^{\ddagger}$(kcal/mol)[b]	ΔG°(kcal/mol)[c]
1	HEH_2/DPPH$^{\bullet}$		1.16	17.36	−16.90
2	1(G)H_2/DPPH$^{\bullet}$	p-OCH_3	1.10×10^{-1}	18.76	−4.70
3		p-CH_3	1.94×10^{-1}	18.42	−4.90
4		p-H	1.66×10^{-1}	18.51	−4.80
5		p-Cl	1.63×10^{-1}	18.52	−4.90
6		p-Br	1.87×10^{-1}	18.44	−4.80
7		p-CF_3	1.26×10^{-1}	18.67	−5.60
8		p-NO_2	1.68×10^{-1}	18.5	−5.40
9	2(G)H_2/DPPH$^{\bullet}$	p-CH_3	6.04×10	15.02	−8.80
10		p-H	8.70×10	14.8	−9.10
11		p-Cl	7.02×10	14.93	−9.40
12		p-Br	8.94×10	14.78	−9.40
13		p-NO_2	8.05×10	14.85	−10.00
14	3(G)H_2/DPPH$^{\bullet}$	p-OCH_3	1.91	17.06	−10.70
15		p-CH_3	1.23×10	15.96	−10.80
16		p-H	9.36	16.12	−11.10
17		p-Cl	4.85	16.51	−11.30
18		p-Br	3.24	16.75	−11.40
19		p-NO_2	2.08	17.01	−12.10
20	4(G)H_2/DPPH$^{\bullet}$	p-OCH_3	2.14×10^2	14.27	−6.30
21		p-CH_3	2.07×10^2	14.29	−6.50
22		p-H	1.74×10^2	14.39	−6.90
23		p-Cl	1.21×10^2	14.61	−7.00
24		p-Br	1.13×10^2	14.64	−7.10
25		p-CF_3	4.03×10^1	15.26	−7.30
26	5H_2/DPPH$^{\bullet}$		1.04×10	16.06	−8.80
27	6H_2/DPPH$^{\bullet}$		5.41	16.45	−7.60
28	7H_2/DPPH$^{\bullet}$		4.87	16.51	−3.50

[a] k_2 is obtained from experimental measurements by a stopped-flow method. The uncertainty is smaller than 5%. [b] $\Delta G^{\ddagger}$ is derived from the Eyring equation $k_2 = (k_B T/h) \exp(-G^{\ddagger}/RT)$. [c] ΔG° is derived from the subtraction of the bond dissociation free energies of two substrates (XH_2 and DPPH$^{\bullet}$): $\Delta G^{\circ} = \Delta G^{\circ}(XH_2) - \Delta G^{\circ}$(DPPHH); the data are obtained from refs 16 and 19b. Reprinted in part with permission from refs 16 and 19b. Copyright 2017 Wiley and 2013 American Chemical Society.

works, the physical significance of thermokinetic parameter $\Delta G^{\ddagger\circ}(XH_2)$ is used to characterize the actual H-donating ability of XH_2 in a HAT reaction during a certain time.[16,18,20,21] The larger the $\Delta G^{\ddagger\circ}(XH_2)$ value is, the weaker the H-donating ability of XH_2 is. Therefore, the order of actual H-donating abilities of these dihydrogen donors is 4(G)H_2 > 2(G)H_2 > 3(G)H_2 (5H_2 > 6H_2 > 7H_2) > HEH_2 > 1(G)H_2. The dihydrogen donors with the strongest H-donating abilities are barbituric acid derivatives 4(G)H_2 (5-benzyl-1,3-dimethylpyrimidine-2,4,6-trione), and the dihydrogen donors with the weakest H-donating abilities are malononitrile derivatives 1(G)H_2 (2-benzylmalononitrile). As the common dihydrogen reducing agent, the ability to release two hydrogen atoms for the Hantzsch ester is not strong among these compounds. Unlike the other seven dihydrogen donors (1H_2−7H_2), the first hydrogen leaving in HEH_2 is the hydrogen attached to the C−H bond, and the second H leaving is attached to N−H bond. However, the leaving of the first H is the rate-determining step of the dihydrogen transfer reaction, so the hydrogen atom on C−H bond plays a decisive role in the dihydrogen transfer reaction rate and the ability of dihydrogen donating for HEH_2. For example, in the synthesis of 1(G)H_2, HEH_2 is usually used as the reducing agent to reduce activated olefins 1(G). In the synthesis of 5H_2, 6H_2, and 7H_2, the C═C bonds in 5−7 activated olefins form $\pi-\pi$ conjugation systems with fluorene groups, which make the C═C bonds difficult to reduce. Therefore, compared with the reduction of olefins 1(G), magnesium perchlorate [$Mg(ClO_4)_2$] needs to be added in the reduction of olefins 5−7 when HEH_2 is used as the reducing agent (Scheme 5a). For olefins 2(G) and 3(G), they are difficult to reduce using HHE_2 as the reductant, and the stronger reductant sodium borohydride ($NaBH_4$) needs to be added (Scheme 5b).

Thermokinetic parameters $\Delta G^{\ddagger\circ}(XH^{\bullet})$ of the active radical intermediates XH$^{\bullet}$ are shown in Scheme 4. The physical significance of the thermokinetic parameter $\Delta G^{\ddagger\circ}(XH^{\bullet})$ is used to characterize the actual H-abstraction ability of XH$^{\bullet}$ in a HAT reaction during a certain time.[16,18,20,21] The greater the negative $\Delta G^{\ddagger\circ}(XH^{\bullet})$ value is, the stronger the H-abstraction ability of

https://doi.org/10.1021/acsomega.2c02264
ACS Omega 2022, 7, 26416−26424

Table 2. Thermokinetic Parameters of XH_2 and $XH^•$, $\Delta G^{‡\circ}(XH_2)$ and $\Delta G^{‡\circ}(XH^•)$, Bond Dissociation Free Energies of XH_2, $\Delta G^\circ(XH_2)$, and Activation Free Energies of Self-Exchange HAT Reactions, $\Delta G^{‡}_{XH_2/XH^•}$, in Acetonitrile at 298 K (kcal/mol)

			DG(kcal/mol)			
entry	$XH_2/XH^•$		$\Delta G^\circ(XH_2)$[a]	$\Delta G^{‡}XH_2/XH^•$[b]	$\Delta G^{‡\circ}(XH_2)$[c]	$\Delta G^{‡\circ}(XH^•)$[d]
1	$HEH_2/HE^•$		63.80	30.25	47.03	−16.78
2	$1(G)H_2/1(G)H^•$	*p*-OCH_3	76.00	20.85	48.43	−27.58
3		*p*-CH_3	75.80	20.37	48.09	−27.72
4		*p*-H	75.90	20.45	48.18	−27.73
5		*p*-Cl	75.80	20.57	48.19	−27.62
6		*p*-Br	75.90	20.31	48.11	−27.80
7		*p*-CF_3	75.10	21.57	48.34	−26.77
8		*p*-NO_2	75.30	21.03	48.17	−27.14
9	$2\ (G)H_2/2(G)H^•$	*p*-CH_3	71.90	17.47	44.69	−27.22
10		*p*-H	71.60	17.33	44.47	−27.14
11		*p*-Cl	71.30	17.89	44.60	−26.71
12		*p*-Br	71.30	17.59	44.45	−26.86
13		*p*-NO_2	70.70	18.33	44.52	−26.19
14	$3(G)H_2/3(G)H^•$	*p*-OCH_3	70.00	23.45	46.73	−23.28
15		*p*-CH_3	69.90	21.35	45.63	−24.28
16		*p*-H	69.60	21.98	45.79	−23.81
17		*p*-Cl	69.40	22.95	46.18	−23.23
18		*p*-Br	69.30	23.53	46.42	−22.89
19		*p*-NO_2	68.60	24.75	46.68	−21.93
20	$4(G)H_2/4(G)H^•$	*p*-OCH_3	74.40	13.47	43.94	−30.47
21		*p*-CH_3	74.20	13.71	43.96	−30.25
22		*p*-H	73.80	14.31	44.06	−29.75
23		*p*-Cl	73.70	14.85	44.28	−29.43
24		*p*-Br	73.60	15.01	44.31	−29.30
25		*p*-CF_3	73.40	16.46	44.93	−28.47
26	$5H_2/5H^•$		71.90	19.55	45.73	−26.18
27	$6H_2/6H^•$		73.10	19.13	46.12	−26.99
28	$7H_2/7H^•$		77.20	15.15	46.18	−31.03

[a] $\Delta G^\circ(XH_2)$ is the bond dissociation free energy of the blue C−H bond.[19] Reprinted in part from ref 19b. Copyright 2013 American Chemical Society. [b] $\Delta G^{‡}_{XH_2/XH^•}$ is the activation free energy of the self-exchange HAT reaction ($XH_2 + XH^• \rightarrow XH^• + XH_2$), which is derived from eq 5. [c] $\Delta G^{‡\circ}(XH_2) = 1/2[\Delta G^{‡}_{XH_2/XH^•} + \Delta G^\circ(XH_2)]$. [d] $\Delta G^{‡\circ}(XH^•) = 1/2[\Delta G^{‡}_{XH_2/XH^•} - \Delta G^\circ(XH_2)]$.

$XH^•$ is. Hence, for these 28 active free-radical intermediates, $4(OH_3)H^•$ [$\Delta G^{‡\circ}(XH^•) = -30.47$ kcal/mol] is the strongest H acceptor and $HEH^•$ [$\Delta G^{‡\circ}(XH^•) = -16.78$ kcal/mol] is the weakest H acceptor. Different from the scales of $\Delta G^{‡\circ}(XH_2)$ for dihydrogen donors, the scales of $\Delta G^{‡\circ}(XH^•)$ for free radicals are quite wide (13.69 kcal/mol). Therefore, the H-abstraction abilities of these radical intermediates vary greatly.

Comparison of Thermokinetic Parameter $\Delta G^{‡\circ}(XH_2)$, Self-Exchange HAT Activation Free Energy $\Delta G^{‡}_{XH_2/XH^•}$, and Bond Dissociation Free Energy $\Delta G^\circ(XH_2)$ of Dihydrogen Donors XH_2. In Scheme 6, $\Delta G^{‡\circ}(XH_2)$, $\Delta G^{‡}_{XH_2/XH^•}$, and $\Delta G^\circ(XH_2)$ of these eight dihydrogen donors without substituents are displayed in one scheme. As is well-known, the bond dissociation free energy $\Delta G^\circ(XH_2)$ is usually used to access the potential H-donating capacity of dihydrogen donor. The bigger the value of $\Delta G^\circ(XH_2)$ is, the weaker H-donating capacity of XH_2 is. It is not difficult to see from Scheme 6a that the potential H-donating capacities of these eight dihydrogen compounds are in the order of $HEH_2 > 3H_2 > 2H_2 > 5H_2 > 6H_2 > 4H_2 > 1H_2 > 7H_2$. Actually, the order of actual H-donating abilities of these eight compounds is provided by thermokinetic parameters $\Delta G^{‡\circ}(XH_2)$ is $4H_2 > 2H_2 > 5H_2 > 3H_2 > 6H_2 > 7H_2 > HEH_2 > 1H_2$ in Scheme 6c. By comparing Scheme 6a and 6c, the actual H-donating ability of dihydrogen donor in HAT reactions is inconsistent with the potential H-donating capacity provided by thermodynamic parameter $\Delta G^\circ(XH_2)$. The reason is that $\Delta G^\circ(XH_2)$ only evaluates the H-donating capacity of the hydrogen donor from the direction of thermodynamics, without considering the kinetic factor of XH_2 in the process of HAT. The activation free energy of the self-exchange HAT reaction $\Delta G^{‡}_{XH_2/XH^•}$, namely the internal kinetic resistance energy of XH_2 in HAT reaction, is listed in Scheme 6b. The bigger the value of $\Delta G^{‡}_{XH_2/XH^•}$ is, the bigger the intrinsic kinetic resistance barrier of XH_2 in HAT reaction is, and the more difficult hydrogen atom donation in kinetics is. In terms of intrinsic kinetic resistance, the order of H-donating

https://doi.org/10.1021/acsomega.2c02264
ACS Omega 2022, 7, 26416−26424

Scheme 3. Visual Comparison of $\Delta G^{\ddagger\circ}(XH_2)$ among the 28 Well-Known Dihydrogen Donors (XH_2) in Acetonitrile at 298 K (kcal/mol)

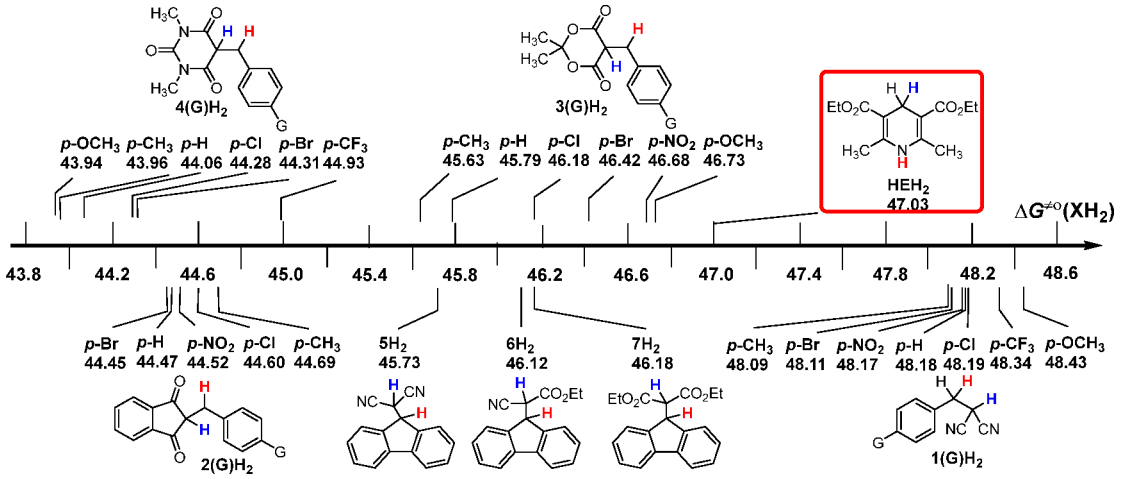

Scheme 4. Visual Comparison of $\Delta G^{\ddagger\circ}(XH^{\bullet})$ among the 28 Well-Known Hydrogen Atom Acceptors ($XH^{\bullet}$) in Acetonitrile at 298 K (kcal/mol)

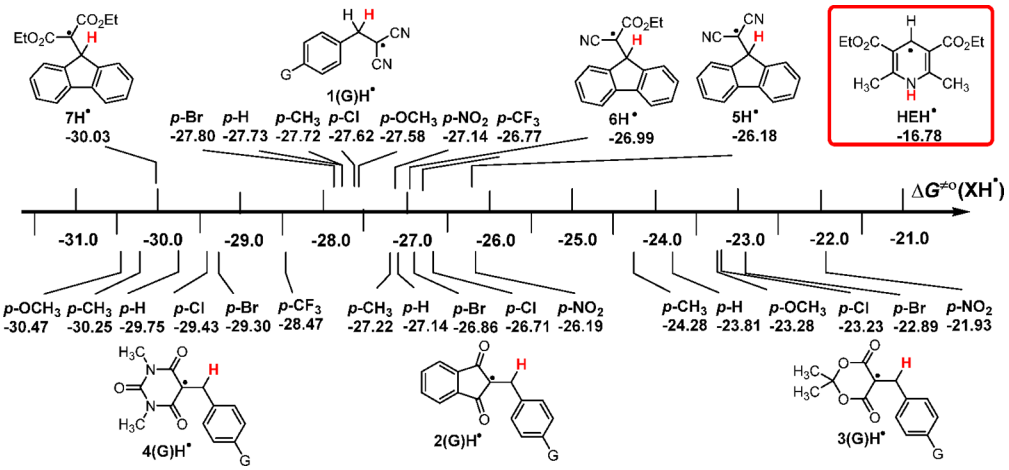

Scheme 5. (a) Reduction of C═C Bonds in Olefins 5−7. (b) Reduction of C═C Bonds in Olefins 2 and 3

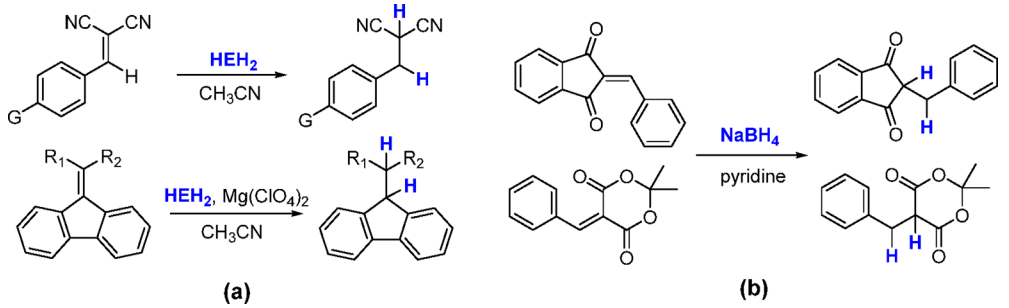

abilities is $4H_2 > 7H_2 > 2H_2 > 6H_2 > 5H_2 > 1H_2 > 3H_2 > HEH_2$. Considering the bond dissociation free energy in thermodynamics and intrinsic kinetic resistance in kinetics of H-donating for XH_2, the actual H-donating ability of dihydrogen donor can be explained.

For HEH_2, although it is the best hydrogen donor in terms of thermodynamics, its actual H-donating ability in HAT reaction is weak due to its maximum intrinsic kinetic resistance for hydrogen donation. For $5H_2$, $6H_2$, and $7H_2$, all three compounds contain fluorene rings. The only differences among them are the groups beside the active hydrogen atoms (the blue hydrogen atoms). The order of the bond dissociation free energies [$\Delta G^{\circ}(XH_2)$, $5H_2 > 6H_2 > 7H_2$] and intrinsic kinetic resistances ($\Delta G^{\ddagger}_{XH_2/XH^{\bullet}}$, $7H_2 > 6H_2 > 5H_2$) of H-donating of these three compounds are opposite. However, the bond dissociation free energies become the main factor affecting the actual H-donating abilities since these three dihydrogen donors have similar structures and small differences in intrinsic kinetic resistances. For $2H_2$, $3H_2$, and $4H_2$, all three compounds are β-dicarbonyl compounds, but the carbon framework rings containing active

https://doi.org/10.1021/acsomega.2c02264
ACS Omega 2022, 7, 26416−26424

Scheme 6. Visual Comparison of (a) $\Delta G^{\circ}(XH_2)$, (b) $\Delta G^{\neq}_{XH_2/XH^{\bullet}}$, and (c) $\Delta G^{\ddagger\circ}(XH_2)$ for Eight Dihydrogen Donors (XH_2) in Acetonitrile at 298 K (kcal/mol)

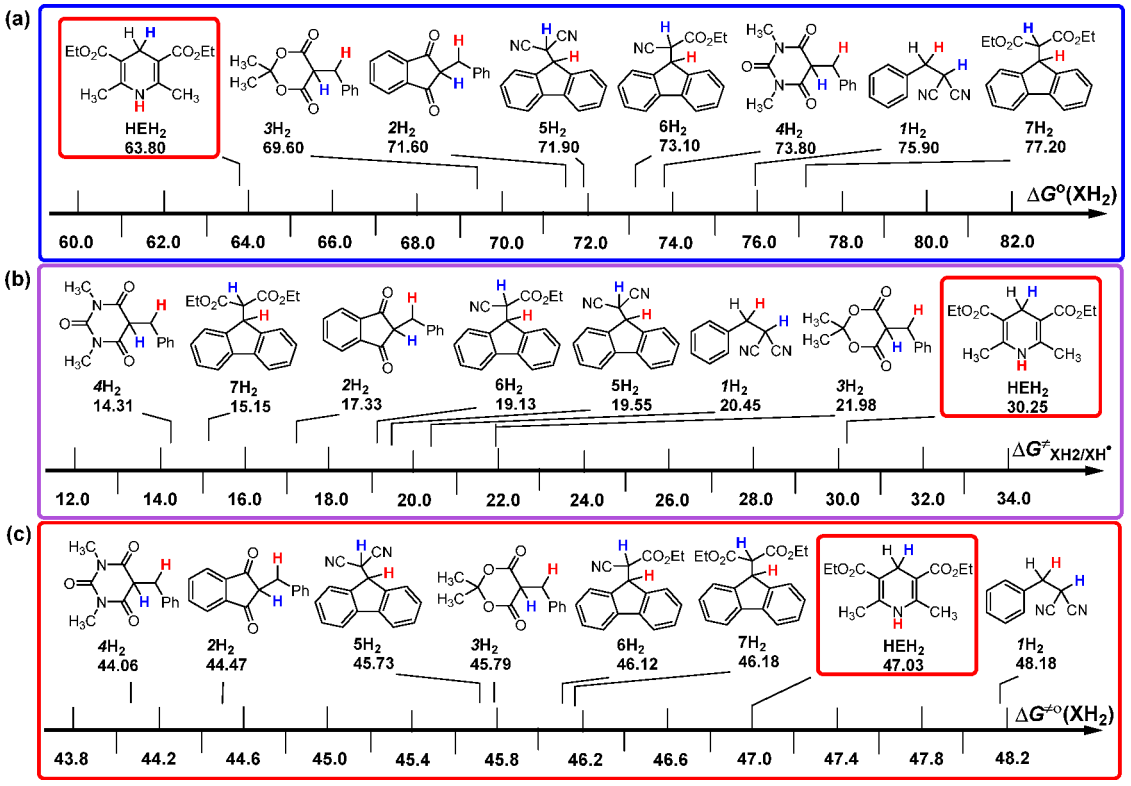

hydrogen atoms are different. The orders of $\Delta G^{\circ}(XH_2)$ ($3H_2$ > $2H_2$ > $4H_2$) and $\Delta G^{\ddagger}_{XH_2/XH^{\bullet}}$ ($4H_2$ > $2H_2$ > $3H_2$) of H-donation for these three compounds are also opposite. However, due to the small difference of bond dissociation free energies among these three compounds, the intrinsic kinetic resistances caused by different structures become the main factor affecting the actual H-donating abilities.

Prediction of the Rate Constants and Verification of the Predictions. In order to investigate the reliabilities of these dihydrogen donors' thermokinetic parameters, HEH_2, $3(G)H_2$, and $4(G)H_2$ are selected to react with 2,4,6-*tert*-butylphenol radical ($^tBu_3PhO^{\bullet}$), and the HAT reaction rate constants are monitored by a stopped-flow method experimentally. According to the thermokinetic parameters of XH_2 in Table 2 and the thermokinetic parameter of $^tBu_3PhO^{\bullet}$ [$\Delta G^{\ddagger\circ}(^tBu_3PhO^{\bullet})$ = −29.56 kcal/mol] determined in previous work,[16] the second-order rate constants of HAT reactions $k_{theor.}$ calculated by thermokinetic parameters of each reactants using eq 4 and Eyring equation, the second-order rate constants measured by experiment $k_{exp.}$, and the $k_{theor.}/k_{exp.}$ are listed in Table 3. Absorbance decay of $^tBu_3PhO^{\bullet}$ at λ_{max} = 631 nm after addition of XH_2 in deaerated anhydrous acetonitrile at 298 K and the fit using the pseudo-first-order kinetic model are listed in the SI. Based on the ratio of $k_{theor.}/k_{exp.}$, the results indicate that the thermokinetic parameters of XH_2 in Table 2 are highly reliable and accurate.

CONCLUSIONS

In this work, the abilities of the Hantzsch ester and other 27 well-known organic dihydrogen donors (XH_2) releasing two hydrogen atoms in acetonitrile at 298 K were identified and researched. The second-order rate constants of 28 HAT reactions between XH_2 and DPPH$^{\bullet}$ in acetonitrile at 298 K were monitored by a stopped-flow method. The thermokinetic parameters of XH_2 and the corresponding radicals $XH^{\bullet}$ were derived according to their definition formulas (eqs 4−6). The reliabilities of the thermokinetic parameters were also examined. The following conclusions can be made:

(1) For these dihydrogen donors, since the transfer processes of the first hydrogen atoms (the blue ones) are the rate-determining steps, the thermokinetic parameters of the first hydrogen atom transfers can represent the abilities of the

Table 3. Comparison of Theoretical k_{HAT} Values of HAT Reactions with the Corresponding Experimental Ones in Acetonitrile at 298 K

entry	$XH_2/^tBu_3PhO^{\bullet}$	k_{theor} (M^{-1} s^{-1})[a]	k_{exp} (M^{-1} s^{-1})[b]	k_{theor}/k_{exp}
1	$HEH_2/^tBu_3PhO^{\bullet}$ $3(G)H_2/^tBu_3PhO^{\bullet}$	9.60×10^{-1}	7.85×10^{-1}	1.22
2	*p*-OCH_3	1.59	1.33	1.20
3	*p*-CH_3	1.02×10	8.58	1.19
4	*p*-Cl	4.03	3.84	1.05
5	*p*-Br	2.69	2.31	1.16
6	*p*-NO_2 $4(G)H_2/^tBu_3PhO^{\bullet}$	1.73	1.09	1.59
7	*p*-OCH_3	1.77×10^2	1.36×10^2	1.30
8	*p*-CH_3	1.71×10^2	1.21×10^2	1.41
9	*p*-H	1.45×10^2	1.07×10^2	1.36
10	*p*-Cl	9.97×10	7.27×10	1.37
11	*p*-Br	9.48×10	6.43×10	1.47
12	*p*-CF_3	3.31×10^2	2.40×10^2	1.38

[a]Derived from $\Delta G^{\ddagger\circ}(XH_2)$ values and $\Delta G^{\ddagger\circ}(^tBu_3PhO^{\bullet})$ according to eq 4. [b]Derived from experimental measurements using the stopped-flow method.

https://doi.org/10.1021/acsomega.2c02264
ACS Omega 2022, 7, 26416−26424

dihydrogen donors releasing two hydrogen atoms. So, unlike other dihydrogen donors ($1H_2$−$7H_2$), even though the first hydrogen release for HEH_2 is attached to C−H, the second H is attached to N−H, and the release of C−H is the rate-determining step of the dihydrogen transfer reaction, which plays a decisive role in the reaction rate and the ability of hydrogen donation.

(2) Thermokinetic parameters $\Delta G^{\ddagger\circ}(XH_2)$ are used to measure the H-donating abilities of eight series of dihydrogen donors with different structures. The $\Delta G^{\ddagger\circ}(XH_2)$ values range from 43.57 kcal/mol for $4(CF_3)H_2$ to 48.43 kcal/mol for $1(OCH_3)H_2$, and the $\Delta G^{\ddagger\circ}(XH^{\bullet})$ values of the corresponding hydrogen atom acceptors ($XH^{\bullet}$) range from −30.47 kcal/mol for $4(OH_3)H^{\bullet}$ to −16.78 kcal/mol for $HEH^{\bullet}$. The order of H-donating abilities for these dihydrogen donors is $4(G)H_2$ > $2(G)H_2$ > $3(G)H_2$ ($5H_2$ > $6H_2$ > $7H_2$) > HEH_2 > $1(G)H_2$.

(3) In terms of bond dissociation free energies $\Delta G^{\circ}(XH_2)$, the order of H-donating abilities of these eight dihydrogen donors is HEH_2 > $3H_2$ > $2H_2$ > $5H_2$ > $6H_2$ > $4H_2$ > $1H_2$ > $7H_2$. In terms of intrinsic kinetic resistance $\Delta G^{\ddagger}_{XH_2/XH^{\bullet}}$, the order of H-donating abilities is $4H_2$ > $7H_2$ > $2H_2$ > $6H_2$ > $5H_2$ > $1H_2$ > $3H_2$ > HEH_2. The order of actual H-donating abilities of these 8 compounds in HAT reactions provided by thermokinetic parameters $\Delta G^{\ddagger\circ}(XH_2)$ is $4H_2$ > $2H_2$ > $5H_2$ > $3H_2$ > $6H_2$ > $7H_2$ > HEH_2 > $1H_2$.

(4) For HEH_2, although it is the best hydrogen donor in terms of thermodynamics, the actual H-donating ability in HAT reaction is weak due to its maximum intrinsic kinetic resistance for hydrogen donation. The H-donating ability of dihydrogen donor is not only related to the bond dissociation free energy $\Delta G^{\circ}(XH_2)$ but also to the intrinsic kinetic resistance $\Delta G^{\ddagger}_{XH_2/XH^{\bullet}}$.

■ ASSOCIATED CONTENT

Supporting Information

The Supporting Information is available free of charge at https://pubs.acs.org/doi/10.1021/acsomega.2c02264.

> Syntheses of HEH_2 and $1H_2$-$7H_2$, and ^1H NMR of the representative compounds, product analysis for the HAT reaction $4H_2$/DPPH$^{\bullet}$ in $CDCl_3$ by ^1H NMR, absorbance decay of $^tBu_3PhO^{\bullet}$ for HAT reactions XH_2/$^tBu_3PhO^{\bullet}$ in acetonitrile at 298 K, and thermodynamic analytic platforms for the reaction mechanisms of XH_2/DPPH$^{\bullet}$ in acetonitrile (PDF)

■ AUTHOR INFORMATION

Corresponding Authors

Yan-Hua Fu − *College of Chemistry and Environmental Engineering, Anyang Institute of Technology, Anyang, Henan 455000, P.R. China;* orcid.org/0000-0001-9321-0805; Email: 20180031@ayit.edu.cn

Guang-Bin Shen − *School of Medical Engineering, Jining Medical University, Jining, Shandong 272000, P.R. China;* orcid.org/0000-0003-0449-7301; Email: gbshen@mail.jnmc.edu.cn

Xiao-Qing Zhu − *Department of Chemistry, Nankai University, Tianjin 300071, P.R. China;* orcid.org/0000-0003-2785-640X; Email: xqzhu@nankai.edu.cn

Authors

Cuihuan Geng − *College of Chemistry and Environmental Engineering, Anyang Institute of Technology, Anyang, Henan 455000, P.R. China*

Kai Wang − *College of Chemistry and Environmental Engineering, Anyang Institute of Technology, Anyang, Henan 455000, P.R. China*

Complete contact information is available at: https://pubs.acs.org/10.1021/acsomega.2c02264

Notes

The authors declare no competing financial interest.

■ ACKNOWLEDGMENTS

Financial support from the PhD Research Startup Foundation of Anyang Institute of Technology (BSJ2019032), the Natural Science Foundation of Henan Province (212300410100), the Research Project of Science and Technology of Henan Province (202102310565), and the Research Project of Science and Technology of Anyang City (2021C01GX004) is acknowledged.

■ REFERENCES

(1) (a) Gong, Q.; Wen, J.; Zhang, X. Desymmetrization of Cyclic 1,3-diketones via Ir-catalyzed Hydrogenation: an Efficient Approach to Cyclic Hydroxy Ketones with a Chiral Quaternary Carbon. *Chem. Sci.* **2019**, *10*, 6350−6353. (b) Shao, Z.; Li, Y.; Liu, C.; Ai, W.; Luo, S.-P.; Liu, Q. Reversible Interconversion between Methanol-diamine and Diamide for Hydrogen Storage Based on Manganese Catalyzed (de)hydrogenation. *Nat. Commun.* **2020**, *11*, 591−597.

(2) (a) Liu, C.; Wang, M.; Xu, Y.; Li, Y.; Liu, Q. Manganese-Catalyzed Asymmetric Hydrogenation of 3H-Indoles. *Angew. Chem.* **2022**, No. e202202814. (b) Yadav, S.; Chaudhary, D.; Maurya, N. K.; Kumar, D.; Ishu, K.; Kuram, M. R. Transfer hydrogenation of pyridinium and quinolinium species using ethanol as a hydrogen source to access saturated N-heterocycles. *Chem. Commun.* **2022**, *58*, 4255−4258.

(3) (a) Yang, J.; Li, X.; You, C.; Li, S.; Guan, Y.-Q.; Lv, H.; Zhang, X. Rhodium-catalyzed Asymmetric Hydrogenation of Exocyclic α,β-unsaturated Carbonyl Compounds. *Org. Biomol. Chem.* **2020**, *18*, 856−859. (b) Bigler, R.; Mack, K. A.; Shen, J.; Tosatti, P.; Han, C.; Bachmann, S.; Zhang, H.; Scalone, M.; Pfaltz, A.; Denmark, S. E.; Hildbrand, S.; Gosselin, F. Asymmetric Hydrogenation of Unfunctionalized Tetrasubstituted Acyclic Olefins. *Angew. Chem., Int. Ed.* **2020**, *59*, 2844−2849. (c) Zhu, L.; Ye, S.; Wang, J.; Zhu, J.; He, G.; Liu, X. Supported Iridium Catalyst for Clean Transfer Hydrogenation of Aldehydes and Ketones using Methanol as Hydrogen Source. *ChemCatChem.* **2022**, *14*, No. e202101794.

(4) Yuan, L.; Shen, G.-B.; Fu, Y.-H.; Zhu, X.-Q. What are the differences between Hantzsch ester and H_2 as two-hydrogen-atom donors in acetonitrile on the thermodynamics of elementary steps? *J. Phys. Org. Chem.* **2017**, *30*, No. e3599.

(5) Shen, G.-B.; Fu, Y.-H.; Zhu, X.-Q. Thermodynamic Network Cards of Hantzsch Ester, Benzothiazoline, and Dihydrophenanthridine Releasing Two Hydrogen Atoms or Ions on 20 Elementary Steps. *J. Org. Chem.* **2020**, *85*, 12535−12543.

(6) (a) Leitch, J. A.; Rogova, T.; Duarte, F.; Dixon, D. J. Dearomative Photocatalytic Construction of Bridged 1,3-Diazepanes. *Angew. Chem., Int. Ed.* **2020**, *59*, 4121−4130. (b) Tang, R.; Shao, Z.; Wang, J.; Liu, Z.; Li, Y.-M.; Shen, Y. Iron(II)-Catalyzed Radical Addition to Aldimines with Hantzsch Ester as a Two-Hydrogen Atom Donor. *J. Org. Chem.* **2019**, *84*, 8177−8184.

(7) (a) Konev, M. O.; Cardinale, L.; Wangelin, A. J. Catalyst-Free N-Deoxygenation by Photoexcitation of Hantzsch Ester. *Org. Lett.* **2020**, *22*, 1316−1320. (b) Zhang, S.; Li, G.; Li, L.; Deng, X.; Zhao, G.; Cui, X.; Tang, Z. Alloxan-Catalyzed Biomimetic Oxidations with Hydrogen

Peroxide or Molecular Oxygen. *ACS Catal.* **2020**, *10*, 245−252. (c) He, W.; Ge, Y.-C.; Tan, C.-H. Halogen-Bonding-Induced Hydrogen Transfer to C = N Bond with Hantzsch Ester. *Org. Lett.* **2014**, *16*, 3244−3247.

(8) (a) Nagode, S. B.; Kant, R.; Rastogi, N. Hantzsch Ester-Mediated Benzannulation of Diazo Compounds under Visible Light Irradiation. *Org. Lett.* **2019**, *21*, 6249−6254. (b) Hamasaka, G.; Tsuji, H.; Ehara, M.; Uozumi, Y. Mechanistic Insight into the Catalytic Hydrogenation of Nonactivated Aldehydes with a Hantzsch Ester in the Presence of a Series of Organoboranes: NMR and DFT Studies. *RSC Adv.* **2019**, *9*, 10201−10210.

(9) (a) Zhu, C.; Saito, K.; Yamanaka, M.; Akiyama, T. Benzothiazoline: Versatile Hydrogen Donor for Organocatalytic Transfer Hydrogenation. *Acc. Chem. Res.* **2015**, *48*, 388−398. (b) Osakabe, H.; Saito, S.; Miyagawa, M.; Suga, T.; Uchikura, T.; Akiyama, T. Enantioselective Dehydroxyhydrogenation of 3-Indolylmethanols by the Combined Use of Benzothiazoline and Chiral Phosphoric Acid: Construction of a Tertiary Carbon Center. *Org. Lett.* **2020**, *22*, 2225−2229.

(10) (a) Li, L.; Guo, S.; Wang, Q.; Zhu, J. Acyl Radicals from Benzothiazolines: Synthons for Alkylation, Alkenylation, and Alkynylation Reactions. *Org. Lett.* **2019**, *21*, 5462−5466. (b) Chen, J.; Huang, W.; Li, Y.; Cheng, X. Visible Light-Induced Difluoropropargylation Reaction with Benzothiazoline as a Reductant. *Adv. Synth. Catal.* **2018**, *360*, 1466−1472.

(11) Chen, Q.-A.; Gao, K.; Duan, Y.; Ye, Z.-S.; Shi, L.; Yang, Y.; Zhou, Y.-G. Dihydrophenanthridine: A New and Easily Regenerable NAD(P)H Model for Biomimetic Asymmetric Hydrogenation. *J. Am. Chem. Soc.* **2012**, *134*, 2442−2448.

(12) Wang, J.; Zhao, Z.-B.; Zhao, Y.; Luo, G.; Zhu, Z.-H.; Luo, Y.; Zhou, Y.-G. Chiral and Regenerable NAD(P)H Models Enabled Biomimetic Asymmetric Reduction: Design, Synthesis, Scope, and Mechanistic Studies. *J. Org. Chem.* **2020**, *85*, 2355−2368.

(13) (a) Luo, Q.; Huang, R.; Xiao, Q.; Kong, L.-B.; Lin, J.; Yan, S.-J. Cascade Reaction of 1,1-Enediamines with 2-Benzylidene-1H-indene-1,3(2H)-diones: Selective Synthesis of Indenodihydropyridine and Indenopyridine Compounds. *ACS Omega* **2019**, *4* (4), 6637−6646. (b) Tan, A.; Kizilkaya, S.; Noma, S. A. A.; Ates, B.; Kara, Y. Novel hybrid isoindole-1,3(2H)-dione compounds containing a 1H-tetrazole moiety: Synthesis, biological evaluation, and molecular docking studies. *J. Biochem. Molecular. Toxicology* **2022**, No. e23015.

(14) (a) Okuno, M.; Yamada, S.; Ohto, T.; Tada, H.; Nakanishi, W.; Ariga, K.; Ishibashi, T. Hydrogen Bonds and Molecular Orientations of Supramolecular Structure between Barbituric Acid and Melamine Derivative at the Air/Water Interface Revealed by Heterodyne-Detected Vibrational Sum Frequency Generation Spectroscopy. *J. Phys. Chem. Lett.* **2020**, *11* (7), 2422−2429. (b) Sepay, N.; Mallik, S.; Guha, C.; Mallik, A. K. An efficient synthesis of 1,3-dimethyl-5-(2-phenyl-4H-chromen-4-ylidene) pyrimidine-2,4,6(1H,3H,5H)-triones and investigation of their interactions with β-lactoglobiulin. *RSC Adv.* **2016**, *6*, 96016−96024.

(15) (a) Wang, X.; Li, J.; Hayashi, Y. Oxidative peptide bond formation of glycine−amino acid using 2-(aminomethyl)malononitrile as a glycine unit. *Chem. Commun.* **2021**, *57*, 4283−4286. (b) Ai, Y.-Y.; Li, D.-A.; Li, G.; Li, H.-P.; He, X.-H.; Fu, X.-J.; Wang, Y.-T.; Zhan, G.; Han, B. Asymmetric Synthesis of Spirocyclopentane Oxindoles via [2 + 3] Annulation with 2-(2-Oxoindolin-3-yl)malononitriles as 1,2-Carbon Bisnucleophiles. *Adv. Synth. Catal.* **2021**, *363*, 3283−3289.

(16) Fu, Y.-H.; Shen, G.-B.; Li, Y.; Yuan, L.; Li, J.-L.; Li, L.; Fu, A.-K.; Chen, J.; Chen, B.-L.; Zhu, L.; Zhu, X.-Q. Realization of Quantitative Estimation for Reaction Rate Constants Using only One Physical Parameter for Each Reactant. *ChemistrySelect* **2017**, *2*, 904−925.

(17) (a) Yeo, J. D.; Shahidi, F. Critical Re-Evaluation of DPPH assay: Presence of Pigments Affects the Results. *J. Agric. Food Chem.* **2019**, *67* (26), 7526−7529. (b) Lee, Y. H.; Chaudhuri, U.; Mahendiran, R. Electrically Detected Paramagnetic Resonance in Ag-Paint-Coated Polycrystalline DPPH. *J. Phys. Chem. C* **2021**, *125* (33), 18438−18443. (c) Zhu, X.-Q.; Zhou, J.; Wang, C.-H.; Li, X.-T.; Jing, S. Actual Structure, Thermodynamic Driving Force, and Mechanism of Benzofuranone-Typical Compounds as Antioxidants in Solution. *J. Phys. Chem. B* **2011**, *115*, 3588−3603. (d) Baliyan, S.; Mukherjee, R.; Priyadarshini, A.; Vibhuti, A.; Gupta, A.; Pandey, R. P.; Chang, C.-M. Determination of Antioxidants by DPPH Radical Scavenging Activity and Quantitative Phytochemical Analysis of Ficusreligiosa. *Molecule* **2022**, *27* (4), 1326−1331.

(18) Zhu, X.-Q.; Deng, F.-H.; Yang, J.-D.; Li, X.-T.; Chen, Q.; Lei, N.-P.; Meng, F.-K.; Zhao, X.-P.; Han, S.-H.; Hao, E.-J.; Mu. Y.-Y. A classical but new kinetic equation for hydride transfer reactions. *Org. Biomol. Chem.* **2013**, *11*, 6071−6089.

(19) (a) Ca, Y. *Hydride Affinities and Heats of Hydrogenation of Organic Unsaturated Compounds Polarized Olefins in Acetonitrile [D]*; Tianjin, Nankai University, 2010. (b) Cao, Y.; Zhang, S.-C.; Zhang, M.; Shen, G.-B.; Zhu, X.-Q. Determination of Thermodynamic Affinities of Various Polar Olefins as Hydride, Hydrogen Atom, and Electron Acceptors in Acetonitrile. *J. Org. Chem.* **2013**, *78*, 7154−7168.

(20) Fu, Y.-H.; Shen, G.-B.; Wang, K.; Zhu, X.-Q. Comparison of Thermodynamic, Kinetic Forces for Three NADH Analogues to Release Hydride Ion or Hydrogen Atom in Acetonitrile. *ChemistrySelect* **2021**, *6*, 8007−8010.

(21) Fu, Y.-H.; Wang, K.; Shen, G.-B.; Zhu, X.-Q. Quantitative comparison of the actual antioxidant activity of Vitamin C. Vitamin E., and NADH. *J. Phys. Org. Chem.* **2022**, No. e4358.

https://doi.org/10.1021/acsomega.2c02264
ACS Omega 2022, 7, 26416−26424